

Self-diffusion and structural properties of confined fluids in dynamic coexistence

N. de Sousa,¹ J.J. Sáenz,^{2,3} Frank Scheffold,⁴ A. García-Martín,⁵ and L. S. Froufe-Pérez⁴

¹*Condensed Matter Physics Center (IFIMAC), Departamento de Física de la Materia Condensada, Universidad Autónoma de Madrid, 28049 Madrid, Spain.*

²*Donostia International Physics Center (DIPC), Paseo Manuel Lardizabal 4, 20018 Donostia-San Sebastian, Spain.*

³*IKERBASQUE, Basque Foundation for Science, 48013 Bilbao, Spain.*

⁴*Department of Physics, University of Fribourg, Chemin du Musée 3, CH-1700, Fribourg, Switzerland.*

⁵*IMM-Instituto de Microelectrónica de Madrid (CNM-CSIC), Isaac Newton 8, PTM, Tres Cantos, E-28760 Madrid, Spain*

(Dated: November 25, 2015)

Self-diffusion and radial distribution functions are studied in a strongly confined Lennard-Jones fluid. Surprisingly, in the solid-liquid phase transition region, where the system exhibits dynamic coexistence, the self-diffusion constants are shown to present up to three-fold variations from solid to liquid phases at fixed temperature, while the radial distribution function corresponding to both the liquid and the solid phases are essentially indistinguishable.

PACS numbers: 82.60.Qr; 05.70.-a; 65.80.-g; 05.70.Fh

I. INTRODUCTION

The thermodynamics and molecular dynamics of gases, liquids, and solids confined to small spaces can differ significantly from the bulk [1, 2]. The confinement of a fluid in a region few times the particle diameter induces density layering and solvation force oscillations [3–5] and can strongly modify the dynamical properties of the fluid [6, 7, 9], such as the diffusion of its constituents [10–14]. The confinement also affects many other macroscopic properties of the fluid [15], from capillary condensation [16, 17] to melting/freezing phase transitions [18–25].

For most liquids, the self-diffusion coefficient in highly confined geometries can decrease (the viscosity can increase) by several orders of magnitude with respect to the macroscopic bulk values [6, 7, 10–14]. Although confinement strongly affects local structuring, the relationships between self-diffusivity and thermodynamic quantities were found to be, to an excellent approximation, independent of the confinement [13, 26], suggesting that thermodynamics can be used to predict how confinement impacts dynamics [27]. More recently, it has been shown that dynamic and equilibrium properties have been explicitly related in supercooled and strongly confined liquids [28]. These findings open an interesting question about the nature of the self-diffusion near the freezing/melting transition in confined geometries. In contrast with macroscopic systems, for small clusters the transition does not take place at a well defined temperature: there is a finite temperature range where solid and liquid phases may coexist dynamically in time [18, 20–22, 29–32], i.e., observing the cluster over a long time, the cluster fluctuates between being entirely solid or liquid.

Numerical simulations have been extensively used to analyze the size dependence of the thermodynamic properties of confined fluids and clusters [18, 21, 22, 33, 34]. Concerning the dynamics and size-dependence of self-diffusion in confined fluids, most of the theoretical work

have been focused on numerical Molecular Dynamics (MD) simulations [10–14, 35, 36]. Dynamic coexistence is not always observed in simulations [37] but the observation of dynamic coexistence will of course depend on the time scale on which dynamic coexistence occurs [32], which can be very large depending on the magnitude of the energy barrier separating the solid and liquid states of the cluster. Dynamic Monte Carlo (DMC) simulations [38] offer an alternative approach that can be used to describe self-diffusion at large time scales [39] where both MD and DMC simulations reveals self-diffusion in confined fluids as a thermal activated process [14].

In this work we analyze and discuss the peculiar behavior of the self-diffusion coefficients and radial distribution function, $g(r)$, in a confined Lennard-Jones in the solid-liquid dynamic coexistence region. We show that the average of the self-diffusion coefficients vary largely from liquid to the solid phase, providing an unambiguous signature of the actual phase state. Interestingly, we find that the $g(r)$ is essentially indistinguishable among both phases. This indicates that the system is in an amorphous solid phase rather than crystal-like. This finding is supported by the observed split-second peak of $g(r)$ which is reminiscent of the behavior observed in nearly jammed disordered hard-sphere packings [40].

II. LENNARD-JONES MODEL

More specifically, we study the self-diffusion coefficient of a medium size (515 atoms) Lennard-Jones (L-J) cluster confined in a spherical cavity as a function of the temperature. In the liquid (fluid-like) phase, just above the melting temperature, the self-diffusion coefficient obtained from DMC numerical simulations follows the typical Arrhenius behavior expected for thermal activated

diffusion. In the coexistence region, the self-diffusion randomly jumps between liquid-like to solid-like reinforcing the relationship between dynamic and thermodynamic properties even in this region. Although the confinement induces a strong anisotropy of the pair-correlation functions of the fluid [41], we find no significant differences in the average radial distribution function between the two phases. Our results suggest that the direct observation of dynamic coexistence could be accessible by experimental approaches sensitive to self-diffusion by Nuclear Magnetic Resonance [42] or Fluorescence Correlation Spectroscopy [43] measurements for instance.

A. Montecarlo simulations

We start by studying a canonical ensemble of point particles interacting through a L-J potential:

$$V_{LJ}(r) = 4\varepsilon \left[\left(\frac{\sigma}{r} \right)^{12} - \left(\frac{\sigma}{r} \right)^6 \right], \quad (1)$$

where ε is the depth of the potential well, r is the distance between particles and σ is the distance at which the inter-particle potential is zero.

The L-J fluid is confined inside a sphere. In order to consider the high possible density in the system, the radius of the confining sphere is chosen in such a way that a highly symmetric portion of a face centered cubic (FCC) lattice fits the spherical volume. To have nearly relaxed structures at zero temperature, the nearest neighbors distance of the FCC lattice is chosen to be $r_m = 2^{\frac{1}{3}}\sigma$.

Throughout this work, unless otherwise specified, we consider 515 particles as can be seen in the sketch of fig. (1). In this figure, the particles are represented by a spheres of radius $r_m/2$, and the translucent sphere represents the confining spherical volume. In an infinite FCC lattice the filling fraction ϕ_∞ is $\phi_\infty \simeq 74\%$. For the case $N = 515$ case studied in this work, we obtain $\phi \approx 56\%$.

In order to generate a suitable statistical ensemble at fixed temperature, we perform standard MC simulations using the canonical ensemble. We depart from a crystalline structure and perform 10^8 of MC steps to thermalise the system. After this process an extensive MC sampling is performed (10^5 configurations, each configuration obtained after 10^5 single-particle MC steps). Temperature and energy is given in units of the potential well.

B. Phase transitions in the system

We determine the temperatures of the (isochore) phase transition in the system by considering the specific heat (SH). The SH C_v is obtained through the fluctuations of the internal energy[44]:

$$C_v(T) = \frac{\partial U(T)}{\partial T} = \frac{\langle E^2 \rangle - \langle E \rangle^2}{T^2}. \quad (2)$$

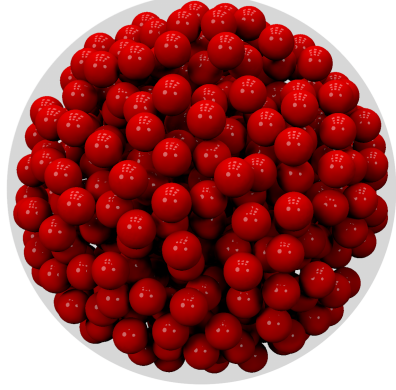


Figure 1. (Color online) Representation of the system under study. The centers of the spheres represent the particles position. The radius of each sphere equals half the L-J potential equilibrium distance $r_m/2$. The translucent sphere represents the confining sphere.

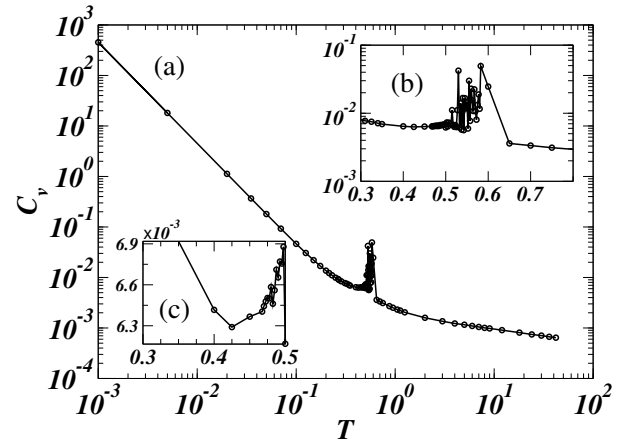


Figure 2. (Color online) Specific heat as function of temperature for a confined L-J system with $N = 515$ particles. Zooms of the specific heat is represent in the box b) and c).

Considering the behavior of the specific heat as function of temperature, as shown in fig. (2a), we observe a high and narrow peak, which we ascribe to a first order phase transition for $T \approx 0.5$. Notice that in the phase transition region we have relevant fluctuations, as can be observed in fig. (2c). Also we observe a modification on SH for temperatures between $0.4 \lesssim T \lesssim 0.5$ (fig. 2b), this feature in the SH might be attributed to a pre-melting region.

In order to better describe the phase transitions in the system, we also estimate the self-diffusion coefficient in the system as a function of the temperature. To do so, the averaged quadratic displacement of particles as function of the performed MC steps were fitted to a linear law

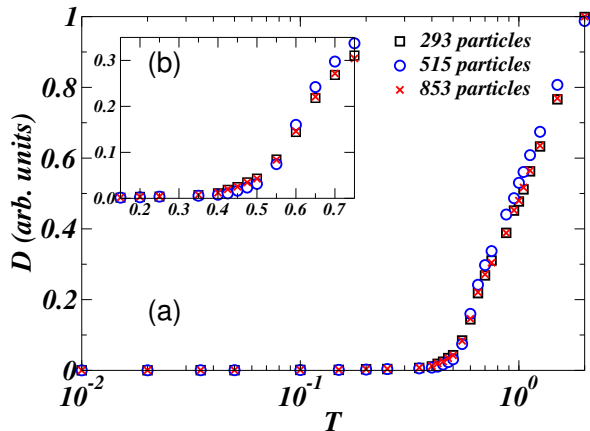


Figure 3. (Color online) a) Diffusion coefficient as a function of the temperature, for three different system sizes of the system at constant particle density. b) Zoom of the same plot in the range $0.15 < T < 0.75$.

(data not shown for the sake of brevity) from whose slope the diffusion coefficient is extracted.

In fig. (3) we plot the diffusion coefficient (D) as a function of temperature for three different systems with different number of particles and different volumes, but obeying to the condition of maximum filling fraction. We observe that the diffusion coefficient, for this scale, does not depend of the size of the system.

Three regions can be identified in fig. (3). In the first region, for normalized temperatures $T \lesssim 0.4$, the structure is crystalline and diffusion is strongly inhibited. This fact is compatible with a pure solid phase. The diffusion coefficient grows with temperature at an approximately constant rate in the range $0.4 \lesssim T \lesssim 0.5$ (See fig. 3b). This apparent increase in D signals a pre-melting. It is worth noticing that this region does not correspond to any remarkable feature in the specific heat. The slope of the diffusion constant shows a strong increase at about $T \simeq 0.5$, this kink in the diffusion coefficient curve corresponds to the peak in the specific heat.

In summary, we can establish a phase landscape in which, we identify a pre-melting region that starts at $T \simeq 0.4$, and a (solid-liquid) phase transition at $T \simeq 0.5$.

III. PHASE SWITCHING

In fig. (4) we represent the particle energy as function of the MC steps for temperature $T = 0.53625$, which corresponds to a temperature in the phase transition region. The system at this temperature oscillates between a lower and a higher value of energy. This bistable energy behavior is the responsible for the fluctuations in the SH. Despite the large number of MC steps used in the sampling, we observe in figure 4 that the number of

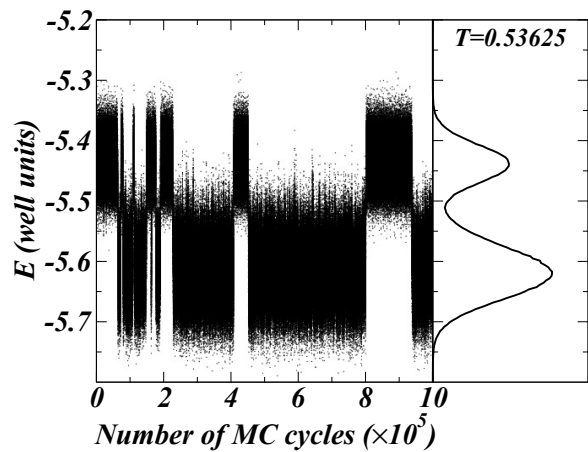


Figure 4. a) Energy sampling of a confined L-J system during a full MC run at a temperature $T = 0.53625$, corresponding to a phase-switching region. b) Energy histogram obtained from the MC sampling in a).

high and low energy regions is relatively reduced. Hence, If we calculate the SH through the energy fluctuations of internal energy, large fluctuations due to finite sampling is expected as observed in fig. (2c).

Representing the internal energy histogram as function of the temperature, shown in fig. (5), we can identify an energy gap for temperatures at the phase transition. The transition between solid and liquid is not smooth with phase coexistence between two states. Instead, the system switches between this two phases, with abrupt modifications in a small number of MC cycles. In the phase transition, when the particles exhibit a low energy configuration, the system is in the solid phase. For higher energies, the system is in the liquid phase. Interestingly, phase coexistence, that might be attributed to intermediate energies in the energy histogram, appear with very low probability as a gap in the distribution.

In order to better understand the geometrical and dynamical properties of the system in the phase switching region, we observe that the system remains in either the lower or the upper energy branches for a sufficient amount of time (MC steps) to consider both the structural (pair correlation function) or dynamical (self-diffusion constant) properties in well defined phases.

A. Dynamical properties in the switching regime

Regarding dynamical properties, in fig. (6c) we plot the self-diffusion constant as a function of energy much in the same way as done in fig. (3). In this case, we have split the statistical ensemble in two different sets for temperatures in the phase switching region, one corresponding to the high energy branch (liquid phase), and the other one corresponding to lower energy branch (solid phase). In fig. (6c) it appears evident that the diffusion

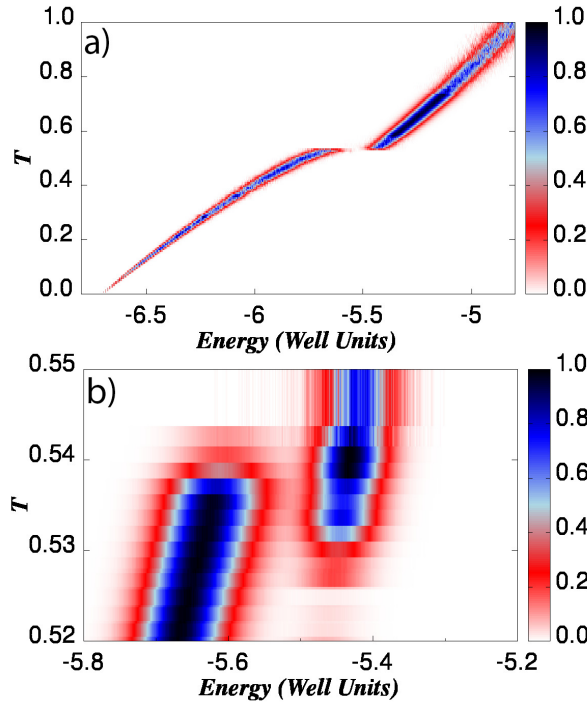


Figure 5. (Color online) a) Colormap showing the energy distribution functions as a function of the temperature. b) Zoom in the region corresponding to the solid-liquid phase transition.

coefficients corresponding to both phases can differ by a large amount. In the case under study, the diffusion constant differs by a factor 3 between phases at the same temperature.

B. Geometrical properties in the switching regime

Regarding geometrical properties of both phases at the phase switching region, we have studied the radial distribution function $g(r)$ [45, 46]. This function is defined as the ratio of the average number density at a distance r from one particle to the averaged number density of an hypothetical, fully uncorrelated, system. Hence, the radial distribution function describes the correlation in the interparticle distance in the system. Again, we can distinguish the statistical sampling in two sets associated with upper and lower energy branches in the phase switching region. Contrary to the behavior of the diffusion constants, the radial distribution function in the upper and lower energy branches is very similar. In Fig. (7) we represent the $g(r)$ for the configurations at both the liquid and solid phase at a fixed temperature. The only marked difference is the indicated split-second peak of $g(r)$ which for bulk packings of hard spheres is a known signature of a solid phase [40, 47]. Other than that the radial distribution functions $g(r)$ remain nearly identical when the switching from solid to liquid phases and a clear

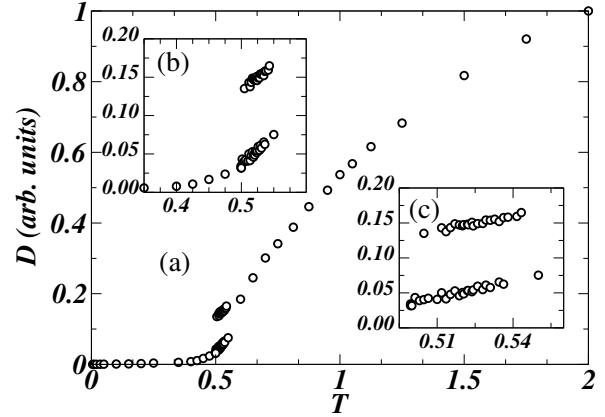


Figure 6. a) Self-diffusion coefficient for a 515 particle system as a function of temperature. b) Zoom of the self-diffusion coefficient in the range $0.35 \leq T \leq 0.6$. c) Self-diffusion coefficients as a function of temperature obtained for the liquid phase (upper branch) and the solid phase (lower branch) in the region of phase-switching.

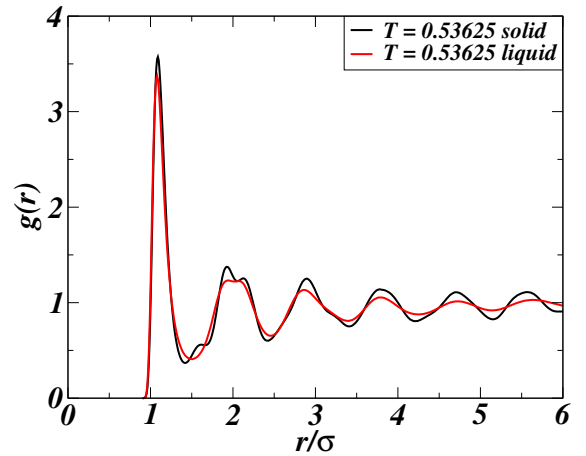


Figure 7. (Color online) Radial distribution function $g(r)$ obtained at a fixed temperature in the phase switching region ($T \simeq 0.53$) for both the solid (black line) and liquid (red line) phases.

identification of different phases through structural measurements is therefore much less sensitive than through dynamical measurements (eg. self-diffusion constants) in strongly confined systems.

IV. CONCLUSION

In summary, we have studied the self-diffusion in a strongly confined Lennard-Jones system. For small clusters, of the order of a few hundreds of particles, instead of phase coexistence the system presents dynamic phase

switching between solid-like and liquid-like amorphous phases. We found that the self-diffusion coefficient of the liquid-like phase in the phase-switching region can be up to a factor of three larger than the one associated to the solid phase. Interestingly, although the radial distribution functions are nearly the same a split-second peak is observed as a subtle structural signature of transient solid phase.

ACKNOWLEDGMENTS

The authors acknowledge Profs. Yuriy G. Pogorelov and Manuel Marqués for useful and stimulating discus-

sions. This research was supported by the Spanish Ministry of Economy and Competitiveness through grant MINIELPHO FIS2012-36113-C03.

REFERENCES

-
- [1] P. Pawlow, *Z. Phys. Chem.* **65**, 1 (1909).
 - [2] T. L. Hill, *Thermodynamics of Small Systems* (Benjamin, New York, 1963).
 - [3] J. P. Hansen, and I. R. McDonald, *Theory of Simple Liquids* (Academic Press, Amsterdam, 2006).
 - [4] J. N. Israelachvili, *Theory of Simple Liquids* (Academic Press, London, 1991).
 - [5] B. Bhushan, J. N. Israelachvili, and U. Landman, *Nature* **374**, 607 (1995).
 - [6] S. Granick, *Science* **253**, 1374 (1991).
 - [7] J. Klein, and E. Kumacheva, *Science* **269**, 816 (1995).
 - [8] D. J. Wales, *Science* **271**, 925 (1996).
 - [9] J. J. Erpenbeck, and W. W. Wood, *Phys. Rev. A* **43**, 4254 (1991).
 - [10] P. A. Thompson, G. S. Grest, and M. O. Robbins, *Phys. Rev. Lett.* **68**, 3448 (1992).
 - [11] J. Gao, W. D. Luedtke, and U. Landman, *Phys. Rev. Lett.* **79**, 705 (1997).
 - [12] J. Mittal, T. M. Truskett, J. R. Errington, and G. Hummer, *Phys. Rev. Lett.* **100**, 145901 (2008).
 - [13] H. Matsubara, F. Pichierri, and K. Kurihara, *Phys. Rev. Lett.* **109**, 197801 (2012).
 - [14] L. D. Gelb, K. E. Gubbins, R. Radhakrishnan, and M. Sliwinski-Bartkowiak, *Rep. on Prog. in Phys.* **62**, 1573 (1999).
 - [15] R. Evans, and P. Tarazona, *Phys. Rev. Lett.* **52**, 557 (1984).
 - [16] M. Köber, E. Sahagún, P. García-Mochales, F. Briones, M. Luna, and J. J. Sáenz, *Small* **6**, 2725 (2010).
 - [17] C. Briant and J. Burton, *J. Chem. Phys.* **63**, 2045 (1975).
 - [18] P. Buffat and J.-P. Borel, *Phys. Rev. A* **13**, 2287 (1976).
 - [19] R. S. Berry, J. Jellinek, and G. Natanson, *Phys. Rev. A* **30**, 919 (1984).
 - [20] J. D. Honeycutt and H. C. Andersen, *J. Phys. Chem.* **91**, 4950 (1987).
 - [21] R. S. Berry, T. L. Beck, H. L. Davis, and J. Jellinek, *Advances in Chemical Physics: Evolution of Size Effects in Chemical Dynamics, Part 2* **70** (John Wiley & Sons, 1988).
 - [22] F. Ercolessi, W. Andreoni, and E. Tosatti, *Phys. Rev. Lett.* **66**, 911 (1991).
 - [23] M. Schmidt, R. Kusche, B. von Issendorff, and H. Haberland, *Nature* **393**, 238 (1998).
 - [24] F. Baletto and R. Ferrando, *Rev. of Mod. Phys.* **77**, 371 (2005).
 - [25] J. Mittal, J. R. Errington, and T. M. Truskett, *Phys. Rev. Lett.* **96**, 177804 (2006).
 - [26] Y. Rosenfeld, *Phys. Rev. A* **15**, 2545 (1977).
 - [27] T. S. Ingebrigtsen, J. R. Errington, T. M. Truskett, and J. C. Dyre, *Phys. Rev. Lett.* **111**, 235901 (2013).
 - [28] P. Labastie and R. L. Whetten, *Phys. Rev. Lett.* **65**, 1567 (1990).
 - [29] D. J. Wales and R. S. Berry, *Phys. Rev. Lett.* **73**, 2875 (1994).
 - [30] C. L. Cleveland, U. Landman, and W. D. Luedtke, *J. Phys. Chem.* **98**, 6272 (1994).
 - [31] D. Schebarchov and S. Hendy, *J. Chem. Phys.* **123**, 104701 (2005).
 - [32] N. Quirke, *Mol. Simulation* **1**, 249 (1988).
 - [33] W. Polak, *European Phys. J. D* **40**, 231 (2006).
 - [34] T. L. Beck and T. L. I. Marchioro, *J. Chem. Phys.* **93**, 1347 (1990).
 - [35] I.-C. Yeh and G. Hummer, *J. Phys. Chem. B* **108**, 15873 (2004).
 - [36] C. L. Cleveland, W. D. Luedtke, and U. Landman, *Phys. Rev. B* **60**, 5065 (1999).
 - [37] D. P. Landau and K. Binder, *A Guide to Monte Carlo Simulation in Statistical Physics* (World Scientific, Singapore, 1994).
 - [38] H. Huitema and J. P. Van der Eerden, *J. Chem. Phys.* **110**, 3267 (1999).
 - [39] M. L. A. Donev, S. Torquato, and F. H. Stillinger, *Phys. Rev. E* **71**, 011105 (2005).
 - [40] K. Nygård, R. Kjellander, S. Sarman, S. Chodankar, E. Perret, J. Buitenhuis, and J. F. van der Veen, *Phys. Rev. Lett.* **108**, 037802 (2012).
 - [41] R. Kimmich, *NMR: tomography, diffusometry, relaxometry* (Springer, Berlin, 1997).
 - [42] E. L. Elson and D. Magne, *Biopolymers* **13**, 1 (1974).
 - [43] F. Wang and D. P. Landau, *Phys. Rev. E* **64**, 056101 (2001).
 - [44] J. K. Percus and G. J. Yevick, *Phys. Rev.* **110**, 1 (1958).
 - [45] M. S. Wertheim, *Phys. Rev. Lett.* **10**, 321 (1963).
 - [46] A. J. Liu, S. R. Nagel, *The Jamming Scenario: An Introduction and Outlook* (Oxford University Press, Oxford, 2010).